PHYSICAL REVIEW A VOLUME 27, NUMBER 5 MAY 1983

# Detailed analysis of the scope of the modified Firsov model

S. A. Cruz* and C. Vargas-Aburto
*Instituto de Física, Universidad Nacional Autónoma de México, Apartado Postal 20-364, Delegación Alvaro Obregón, 01000 México, Distrito Federal, Mexico*

D. K. Brice
*Sandia National Laboratories, Albuquerque, New Mexico 87185*

E. V. Alonso† and D. G. Armour
*Department of Electrical Engineering, University of Salford, Salford M5 4WT, United Kingdom*
(Received 1 April 1982)

A detailed and systematic analysis of the scope of the Firsov model as modified by Cheshire when no adjustable parameters are included in the calculations of the low-velocity electronic-stopping cross section is presented. For this purpose we summarize and extend our previously reported [Radiat. Eff. Lett. 43, 79 (1979); Nucl. Instrum. Methods 170, 205 (1980)] preliminary results on the role of all computational degrees of freedom that influence the outcome of the calculations, namely, (a) inclusion of trajectory, (b) accuracy of wave functions and speed of atomic electrons, (c) motion of Firsov's plane, and (d) consideration of experimental conditions. We find that the Firsov theory is accurate only within a factor of 2; therefore, at least a scale factor is necessary in order to get reasonable agreement with experiment.

## I. INTRODUCTION

This is the last of a series of papers written to study the sensitivity of the modified Firsov model to the different parameters involved in the calculation of the inelastic stopping power of solids and gases.

In the study of the energy lost by ions while traversing matter at relatively low energies, two models have been extensively used in the literature, namely, the Firsov formalism[1] and the Lindhard-Scharff formalism.[2] Both models are based on the electron-gas theory of Thomas and Fermi but differ conceptually in that the Lindhard model considers the projectile as an electric charge moving through an electron gas and therefore the energy loss is evaluated in terms of a drag force exerted by the medium on the projectile. On the other hand, the Firsov formalism considers the collision between two Thomas-Fermi atoms and evaluates the energy loss as due to a drag force produced by electron-electron momentum transfer between both systems. Although the two models provide, on the average, reasonable estimates for the electronic-stopping cross section ($S_e$), the experimentally observed oscillatory behavior of $S_e$ as a function of projectile (target) atomic number cannot be explained by them as they stand, and therefore in the last few years several modifications have been introduced to both in order to account for the atomic structure of the colliding partners.

Land *et al.*[3] have carried out a comparison between the Firsov model as modified by Cheshire[4] and the Lindhard model modified by other authors.[5] They find that in both cases at least one adjustable parameter is necessary in order to get good agreement with experiment. Moreover, they conclude that the predicted values of $S_e$ according to Cheshire's modification are strongly dependent on the choice of a minimum impact parameter involved in the calculations. We have recently found (Refs. 6 and 7, hereafter referred to as I and II) that the Firsov model as modified by Cheshire is highly sensitive to the accuracy of the atomic wave functions as well as to the use of an average rather than an rms speed for the atomic electrons. This fact constitutes an additional computational degree of freedom which should be considered in order to draw any conclusions on the value of any adjustable quantities in the Firsov approach.

In this work we confine ourselves to a detailed and systematic analysis of the scope of the Firsov model as modified by Cheshire when *no adjustable parameters* are included in the calculations of inelastic energy losses and particularly in the evaluation of the electronic-stopping cross section ($S_e$). We investigate also the role of all computational degrees of

 

freedom that influence the outcome of the calculations, namely:

(1) inclusion of the trajectory determined by standard and "realistic" interaction potentials, respectively;

(2) use of accurate atomic wave functions and average speed for the atomic electrons in the evaluation of the momentum exchange between the colliding partners as well as proper location of the region where the momentum exchange is to be evaluated;

(3) consideration of the experimental conditions for the evaluation of the distances of closest approach in multiple-scattering events.

Although the work is mainly devoted to Cheshire's modification, we find it convenient to analyze Brice's modification for the low-velocity region,[8] which, in contrast to the above treatment, is the only approach that evaluates the momentum transfer between projectile and target from a quantum-mechanical viewpoint. Our findings in this case are that Brice's model is not very sensitive to the choice of wave functions, which is the only quantity that could affect its predictions.

For completeness, the original Firsov model and its modification due to Cheshire and Brice, respectively, are briefly reviewed in Sec. II. In Sec. III we analyze in detail the main factors that affect the predictions of the theory for the modifications reviewed in Sec. II. Section IV presents the results of these calculations using the appropriate parameters obtained in a consistent way and a comparison with experimental data from the literature is also shown. Finally, a discussion and the conclusions of the present work are presented in Sec. V. An Appendix is devoted to the inclusion of some detailed calculations at the end of the work.

## II. FIRSOV MODEL AND ITS MODIFICATIONS

### A. Original model

The original model proposed by Firsov[1] for the calculation of the inelastic energy loss is based on the fact that in each individual encounter between the incident beam ions and the target atoms, a deceleration of the incoming particles takes place due to a drag force produced by momentum exchange involving projectile and target electrons. Owing to the indistinguishability of the electron we could regard this momentum exchange as an electron exchange, i.e., as the projectile and target approach each other, their electronic clouds start overlapping and an electron, which originally belonged to one of the systems, suddenly switches its parent atom, carrying with it a momentum $m\vec{u}$ where $m$ is the electron mass and $\vec{u}$ the relative velocity of the two systems. The drag force is then calculated in terms of the flux of momentum due to the electrons of both projectile and target.

If the motion of the electrons is assumed to be governed by the Thomas-Fermi field of the atom, and a hypothetical plane is defined perpendicular to the line joining the nuclei at a certain fixed position dictated by the atomic Thomas-Fermi potential, then an expression for the total flux of electrons across an element of area $dA$ of the plane in one direction is readily obtained as

$$d\phi = \tfrac{1}{4} n \langle v \rangle dA \ , \tag{1}$$

where $n$ and $\langle v \rangle$ are the Thomas-Fermi number density and average speed of the electrons, respectively. The inelastic energy transfer $\epsilon$ in a collision for a given impact parameter $b$, corresponds to the work of slowing down and, within this model, is given by

$$\epsilon(b) = m \int \vec{u} \cdot d\vec{R} \int d\phi \ , \tag{2}$$

where $m$ and $\vec{u}$ have the same meaning as before and $\vec{R}$ is the relative position vector between target and projectile. The electronic-stopping cross section ($S_e$) is defined as the integral

$$S_e = \int_{b_0}^{\infty} db \, 2\pi b \epsilon(b) \ , \tag{3}$$

where the lower limit $b_0$ is necessary to account for the particular experimental conditions[4] (see Sec. IV). The location of the hypothetical plane is normally determined by the region between projectile and target where the electrons "feel" the minimum potential energy. Firsov proposed that for projectile-target combinations not differing by more than a factor of 4 in atomic number, the plane could be positioned half-way between them.[1]

It is evident that the main feature in the Firsov model is the flux evaluation as given by Eq. (1). Since this flux depends directly on the electronic distribution $n$, a corrrelation between the details of the charge distribution and the electronic-stopping power could be expected. In fact, for a Thomas-Fermi atom the electronic distribution does not change appreciably with $Z$,[9] therefore the original Firsov idea as it stands cannot account for the experimentally observed strong variations of $S_e$ as a function of projectile (target) atomic number.[10]

Several authors[4,8,11–13] have properly modified the original model of Firsov in order to explain the structure effects in $S_e$ and, although there exist different versions for such modification, we can essentially group them into two main categories: (1) those approaches which have been made by retaining the idea of the electronic flux as being a classical effusion process, evaluating it through the use of more

accurate descriptions of the electron density and velocity (first proposed by Cheshire *et al.*) and (2) those that have used a quantum-mechanical formulation for the flux evaluation in the spirit of the original Firsov model (first proposed by Brice).

Since these two approaches are substantially different in their formulation, before proceeding any further, we consider it useful to present a brief review of their main assumptions for the sake of completeness.

### B. Cheshire's modification

Cheshire *et al.*[4] evaluated the flux given in Eq. (1) by replacing the Thomas-Fermi density and the average speed by more accurate expressions, namely, the Hartree-Fock wave functions for the atomic electrons and the corresponding rms speed derived from the expectation value of the kinetic-energy operator for any particular orbital. Denoting by $\omega_\lambda$ the population of orbital $\lambda$ then the expression for the flux [Eq. (1)] due to this orbital is

$$d\phi_\lambda = \tfrac{1}{4}\omega_\lambda \psi_\lambda \psi_\lambda^* \langle v_\lambda^2 \rangle^{1/2} . \tag{4}$$

The corresponding expression for the rms speed of orbital $\lambda$, in terms of the kinetic-energy operator $\hat{T}$, is

$$\langle v_\lambda^2 \rangle^{1/2} = (2/m)^{1/2} \left[ \int \psi_\lambda^* \hat{T} \psi_\lambda d\tau \right]^{1/2} . \tag{5}$$

Following the idea of rectilinear trajectories as in the original Firsov model, Cheshire retained the notion of a minimum impact parameter in Eq. (3). In addition to this a new variable was introduced in order to account for the position of the hypothetical plane through which the flux was to be evaluated. By considering the degree of nuclear screening for systems with different electronic structure, the location of the plane was set at the point where the colliding atoms make equal contributions to the electrostatic potential.

Using Eqs. (4) and (5) into Eq. (2) and integrating over the hypothetical surface, Cheshire's result for the contribution to $\epsilon(b)$ from orbital $\lambda$ of either projectile or target is

$$\epsilon_\lambda(b) = \pi m u \omega_\lambda (1/\alpha) \langle v_\lambda^2 \rangle^{1/2} I(\alpha b) , \tag{6}$$

with

$$I(\alpha b) = \int_{\alpha b}^{\infty} \psi_\lambda^* \psi_\lambda r (r^2 - \alpha^2 b^2)^{1/2} dr . \tag{7}$$

The dimensionless quantity $\alpha$ represents the fractional position of the hypothetical surface between the incident particle and the target. The electronic-stopping cross section is readily obtained from Eq. (3), once a minimum impact parameter is determined. This last quantity has been considered as an adjustable parameter[3] and it will be a subject of further discussion later in this work.

### C. Brice's modification

As the reader must be aware, Cheshire's modification is basically a semiclassical approach in which the central feature of the original model is retained in its essence, i.e., the flux is calculated as given by Eq. (1). A substantially different treatment to the flux evaluation was first introduced by Brice,[8] who described the rate of momentum transfer between projectile and target in terms of the quantum probability current across the plane in one direction. For this purpose, Brice defined a partial wave function (PWF) as

$$\Lambda_+(\vec{r}') = (1/2\pi)^{3/2} \int_{-\infty}^{\infty} dk_x \int_{-\infty}^{\infty} dk_y \int_{k_0}^{\infty} dk_z e^{i\vec{k}\cdot\vec{r}'} \Phi(\vec{k}) , \tag{8}$$

where $\vec{r}'$ is a point on the plane relative to one of the colliding partners and $\Phi(\vec{k})$ the Fourier transform of the electronic wave function for a given orbital. The motion of the plane, as projectile and target approach each other, is accounted for by $k_0$. A direct consequence of this is that the PWF will only consider those electrons whose velocity allows them to reach the plane and hence contribute to the flux. In terms of the PWF the flux is given as

$$\phi = -\frac{i\hbar}{2m} \int \left[ \Lambda_+^* \frac{\partial \Lambda_+}{\partial z} - \Lambda_+ \frac{\partial \Lambda_+^*}{\partial z} - 2ik_0 |\Lambda_+|^2 \right] dx\, dy . \tag{9}$$

Using this expression in Eq. (3) and integrating over all impact parameters (including the zero value), the low-energy contribution to the electronic-stopping cross section becomes[14]

$$S_e = -8\pi\hbar u \int dk_x \int dk_y \int dk_z k_z \left| \frac{\partial \Phi}{\partial z} \right|^2 , \qquad u \ll e^2/\hbar . \tag{10}$$

It is worth mentioning at this stage that Eq. (10) is the lowest-order term to a more general dependence of $S_e$ on $u$ (see Ref. 8). Equation (10) gives the explicit dependence of $S_e$ on the electron distribution through $\Phi(\vec{k})$. Originally, Brice employed simple hydrogenic orbitals to obtain a closed expression for $S_e$ as

$$S_e = -128(N_1+N_2)\hbar u a_0/15Z_{\text{eff}} , \quad (11)$$

with $N_1,N_2$ the number of electrons for projectile and target, respectively, and $Z_{\text{eff}}$ a parameter adjustable to experiment; $a_0$ is the Bohr radius. More recently, it has been shown[14] that the $Z_{\text{eff}}$ parameter is obtained from first principles when more realistic descriptions for the atomic wave functions are used.

## III. DETAILED ANALYSIS

A first look at Eq. (7) could lead us to conclude that the only degrees of freedom introduced in the computation of $S_e$ are contained in the parameters $\alpha$ and $b$. However, it has been shown in I and II that Cheshire's modification is extremely sensitive to the accuracy of the electronic wave functions and to the way in which the average speed of atomic electrons is described. In this section we make an exhaustive analysis of all the factors that influence the predicted values for $S_e$ according to Cheshire's modification.

### A. Sensitivity to the atomic wave functions

The original Firsov model contemplates the electronic distribution of the colliding partners as due to the free Thomas-Fermi atoms. If we are to consider, however, the detailed electronic structure of projectile and target, we must establish the limits to which such a study must be carried out within the spirit of the original model. From this point of view, since the Firsov model was originally designed to describe changes in internal energy of the colliding partners on a statistical basis, i.e., assuming a continuous distribution of electronic energy states, we shall not attempt to account for effects of a pure quantum origin such as inner-shell promotion mechanisms or processes requiring a more fundamental analysis based on molecular-orbital theory.[15] We shall, therefore (consistent with the fundamental Firsov concept), consider that the atomic structure of projectile and target can be described by the free-atom spatial electronic distribution. For solid targets we expect that the electronic distributions are different from those in the free-atom case; however, we shall still consider the free-atom wave functions as a reasonable description in order to explore the scope and predictions of the Firsov model.

Let us describe an atomic orbital as the linear combination of Hartree-Fock-Slater (HFS) orbitals:

$$\psi_\lambda(\vec{r}) = \sum_p C_p r^{n_p-1} e^{-\xi_p r} Y_\lambda^\mu(\hat{r}) , \quad (12)$$

where

$$C_p = [(2\xi_p)^{2n_p+1}/(2n_p)!]^{1/2} a_p , \quad (13)$$

and $a_p,\xi_p,n_p$ are tabulated quantities given by Clementi *et al.*,[16] $Y_\lambda^\mu$ being the usual spherical harmonics.[17] Regarding the rectilinear trajectory approximation, and in terms of these last two expressions, it may be easily shown that Eq. (7) becomes

$$I(\alpha b) = (1/4\pi)\sum_{p,q} C_p C_q \int_{\alpha b}^{\infty} r^{\nu-1} e^{-\eta r}(r^2-\alpha^2 b^2)^{1/2} dr , \quad (14)$$

with

$$\nu = n_p + n_q , \quad \eta = \xi_p + \xi_q . \quad (15)$$

Although the integrals that appear in Eq. (14) may be evaluated analytically, it is convenient to retain their explicit expression for all practical purposes (see below). The contribution to $S_e$ from orbital $\lambda$ of either projectile or target is obtained by substituting Eq. (14) into Eqs. (2) and (3) which after little manipulation becomes

$$S_e^\lambda = (\pi m u/2\alpha)\omega_\lambda \langle v_\lambda^2 \rangle^{1/2} \sum_{p,q} C_p C_q \alpha^{\nu+1} b_0^{\nu+3} e^{-\gamma} J(\nu,\gamma;\beta) , \quad (16)$$

where

$$J(\nu,\gamma;\beta) = \int_0^\infty (\beta+1)^{\nu+2} e^{-\gamma\beta} \left[ \int_0^\infty (\rho+1)^{\nu-1} e^{-(\beta+1)\gamma\rho} (\rho^2+2\rho)^{1/2} d\rho \right] d\beta \quad (17)$$

and the following definitions hold:

$$\gamma = \eta\alpha b_0 , \quad \beta = b/b_0 - 1 , \quad \rho = r/\alpha b_0 - 1 , \quad (18)$$

$\nu$ and $\eta$ being given by Eq. (15). The integrals $J(\nu,\gamma;\beta)$ have been evaluated numerically in I and II using a 15-point Gauss-Laguerre procedure.

Several authors have used a minimal-basis representation for the atomic orbitals in Eq. (16) and it has normally been accepted that the predicted values of $S_e$ within this representation are reasonably good. However, when more accurate wave functions are used, a strong dependence of the predicted values for $S_e$ on the choice of basis set is observed as shown in Fig. 1, where we plot $S_e$ for different neutral projectiles incident on carbon ($v = 0.50 v_0$) using different degrees of accuracy for the wave functions into Eq. (16).

The major problem with the minimal-basis set is that it yields a reasonable value for the energy of the atomic orbitals while providing an inadequate

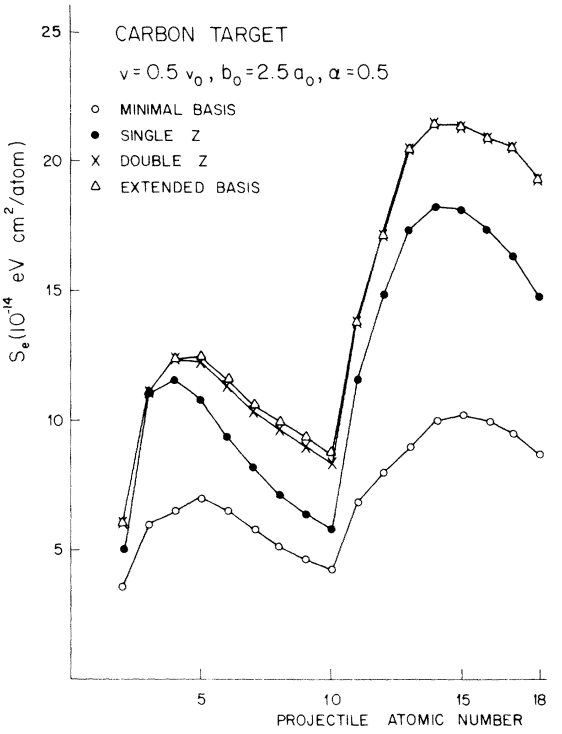


FIG. 1. Sensitivity of the predicted values of $S_e$ to the choice of basis set using the rms speed for the electrons and the rectilinear trajectory approximation.

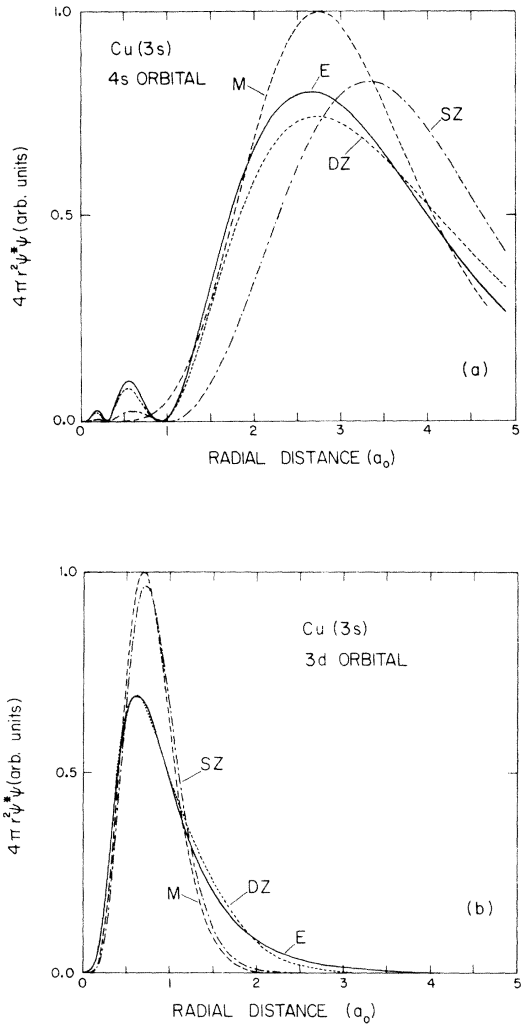


FIG. 2. Radial charge distribution of some orbitals of Cu(3*S*) calculated with different accuracies for the electronic wave function. (*M*) minimal basis, (*SZ*) single zeta, (*DZ*) double zeta, (*E*) extended: (a) 4*s* orbital, (b) 3*d* orbital.

description of the electronic distribution. This, together with the orbital velocity, represents the determining factor in the evaluation of the flux using Cheshire's treatment. The effect of the choice of basis set on the electronic distribution is illustrated in Figs. 2(a) and 2(b) where the radial charge distributions of the 4*s* and 3*d* orbitals in Cu(3*S*), calculated using a minimal (*M*), single-zeta (*SZ*), double-zeta (*DZ*), and extended (*E*) basis set, are plotted. The shift in the maximum for the radial charge distributions as a function of the accuracy of the wave function is clearly observable. The less accurate wave function tends to describe poorly the shape and extent of the most external orbitals, which happen to be the most important in the evaluation of $S_e$.[14] It can thus be expected that part of the discrepancy in the theoretically predicted values for $S_e$ when using different degrees of accuracy is due to their different description of the electronic density.

Let us concentrate for the moment, on the integrals $I(\alpha b)$ appearing in Eq. (14). As pointed out by Komarov *et al.*[18] these integrals correspond to an "incomplete and distorted normalization" of the wave function, the degree of distortion being governed by the product $\alpha b$ (note that this product also appears in the limits of integration). Figure 3 shows a plot of $I(\alpha b)$ for the various basis sets for the case of the 3*d* orbital of Cu(3*S*). The strong dependence on the choice of accuracy for the wave function is evident at the larger values of $\alpha b$. Moreover, we could match the values of $I(\alpha b)$ for the minimal- and extended basis set by choosing different values for product $\alpha b$ in the two cases. This explains why the use of accurate wave functions in the calculation of such integrals demands a different value for $\alpha b$ with respect to the calculations that employ minimal-basis sets. This is partly responsible for the fact that some authors have used *ad hoc* minimum impact parameters in their calculations.[3,18]

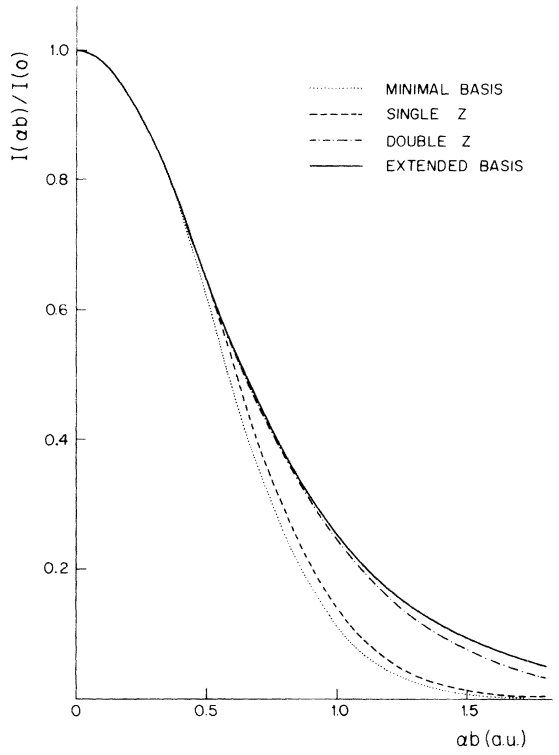


FIG. 3. Behavior of the integrals $I(\alpha b)$ [Eq. (14)] as a function of $\alpha b$ for different accuracy of the wave functions (see text).

TABLE I. Brice's $Z_{\text{eff}}$ parameter for some ion-target combinations.[a]

| Projectile \ Target | C | Ne | Rb |
|---|---|---|---|
| $C^+$ | 1.530 | 2.010 | 1.872 |
| | (1.469) | (1.962) | (1.764) |
| $Ne^+$ | 1.871 | 2.291 | 1.977 |
| | (1.804) | (2.242) | (1.867) |
| $Rb^+$ | 1.974 | 2.134 | 1.999 |
| | (1.947) | (2.116) | (1.926) |

[a]Values in parentheses obtained with minimal-basis sets (see text).

So far we have found that the apparent sensitivity of Cheshire's approach to the type of wave functions is mainly due to the extension of the electronic distribution and the accuracy with which this can be described. Interestingly enough, Brice's treatment is not appreciably sensitive to the choice of wave functions. Table I shows the value for Brice's $Z_{\text{eff}}$ parameter for different basis sets in a few cases. As can be seen, very little difference is found ($\sim 5\%$) between the values obtained using a minimal-basis set and an extended basis.

### B. Sensitivity to the average speed of atomic electrons

In their modification to the original Firsov model, Cheshire *et al.* and other authors[3,11–13,18] replaced, for simplicity, the Thomas-Fermi average speed of the electrons by the Hartree-Fock rms speed [see Eq. (5)]. Although for a classical gas of particles we may expect no strong variations between average and rms speed, for an electron gas the differences are quite important[19] and, as a consequence, the predicted values of $S_e$ must depend strongly on the use of $\langle v \rangle$ rather than $\langle v^2 \rangle^{1/2}$ in Eqs. (6) and (16). We have shown in II that this is indeed the case and in this section a detailed analysis of the reasons for such a behavior is presented.

The average speed for a given atomic orbital is given by

$$\langle v_\lambda \rangle = (\hbar/m) \int \Phi_\lambda^*(\vec{k}) \, | \, \vec{k} \, | \, \Phi_\lambda(\vec{k}) d\tau_k \ , \tag{19}$$

where $\Phi_\lambda(\vec{k})$ is the Fourier transform for orbital $\psi_\lambda(\vec{r})$ [see Eq. (12)], which explicitly reads as[14]

$$\Phi_\lambda(\vec{k}) = (2/\pi)^{1/2} i^\lambda \lambda! (2k)^\lambda Y_\lambda^u(\hat{k}) \sum_p (-1)^{n_p} C_p \frac{\partial^{n_p-\lambda}}{\partial \xi_p^{n_p-\lambda}} (k^2+\xi_p^2)^{-\lambda-1} \ . \tag{20}$$

Substitution of Eq. (20) into Eq. (19), together with appropriate manipulation (see the Appendix), yields the following expression for the average speed (in units of $v_0$):

$$\langle v_\lambda \rangle = 4(\lambda+1)! \left[ 2^{2\lambda+1}(\lambda!) \sum_{p,q} (-1)^{n_p+n_q+1} C_p C_q \xi_p D^{n_p-\lambda-1, n_q-\lambda} I(\lambda, \lambda+2, \lambda+1; \xi_p^2, \xi_q^2) \right.$$
$$\left. + \sum_p C_p^2 \sum_{g,h} K(n_p, g, h; \lambda) \xi_p^{-2n_p} \right] , \tag{21}$$

with $I(\lambda,\lambda+2,\lambda+1; \xi_p^2, \xi_q^2)$ and $K(n_p,g,h;\lambda)$ given in the Appendix by Eqs. (A5) and (A9), respectively. $D^{a,b}$ is

a differentation operator defined as[14]

$$D^{a,b}=\frac{\partial^a}{\partial\xi_p^a}\frac{\partial^b}{\partial\xi_q^b}\ . \tag{22}$$

On the other hand, introducing Eq. (12) into Eq. (5), the following expression for $\langle v^2\rangle^{1/2}$ is obtained:

$$\langle v_\lambda^2\rangle^{1/2}=2^{1/2}\sum_{p,q}C_pC_q(\nu-2)!\eta^{-\nu-1}\{[\lambda(\lambda+1)-n_q(n_q-1)]\eta^2+\nu\xi_q[2\xi_pn_q-\xi_q(n_p-n_q-1)-2\xi_qn_q\eta]\}\ , \tag{23}$$

with $\eta,\nu$ defined by Eq. (15).

Table II shows a comparison between the values of $\langle v_\lambda\rangle$ and $\langle v_\lambda^2\rangle^{1/2}$ as evaluated through Eqs. (21) and (22), respectively, for selected orbitals of some atoms and ions. It is now evident that the large differences observed between the average and rms speed make Eq. (16) a highly sensitive function of the choice of speed. Therefore in accordance with the original theory, it is important that the average speed is used. Moreover, Table III shows, as expected, that the values of $\langle v_\lambda\rangle$ (and $\langle v_\lambda^2\rangle^{1/2}$) are strongly dependent on the accuracy of atomic wave function. As an example, the $\langle v\rangle$ and $\langle v^2\rangle^{1/2}$ for the $3s$, $3p$, $3d$, and $4s$ orbitals of Cu($3S$) are shown in this table.

These results, together with those of Sec. III, underline the importance of employing both the accurate wave functions and the average speed for the atomic electrons through all the calculations, if the Firsov model as modified by Cheshire is to be used in a consistent way.

### C. Importance of the trajectory and position of the Firsov plane

Up to this moment we have shown explicitly the importance of the choice of wave functions in the evaluation of $S_e$ within Cheshire's modification to the Firsov model. Moreover, the use of the accurate wave functions together with the average speed for the electrons removes the major inconsistencies which had always been present in such calculations. However, as pointed out before, all the previous discussion is based on the assumption of a rectilinear trajectory for the projectile. We shall now analyze how important the inclusion of the trajectory is in the calculations of the inelastic energy loss in a single collision to draw any conclusions on the validity of the rectilinear trajectory approximation.

In order to evaluate the integral given by Eq. (2) along the path, let us assume that the inelastic energy loss is small as compared to the total energy and hence treat the trajectory as the elastic one, i.e., a typical central-force problem.[20] The term $\vec{u}\cdot d\vec{R}$ in Eq. (2) may be related to the dynamical variables through the orbit equation and it may be shown that

$$\vec{\mu}\cdot d\vec{R}=\frac{\mu_0(1-V(R)/E_{\rm rel})dR}{[1-V(R)/E_{\rm rel}-b^2/R^2]^{1/2}}\ , \tag{24}$$

where $\mu_0$ is the projectile speed in the laboratory frame, $b$ the impact parameter, and $V(R)$ the pairwise interatomic potential between projectile and target. $E_{\rm rel}$ stands for the relative kinetic energy:

$$E_{\rm rel}=E_0m_p/(m_p+m_T)\ , \tag{25}$$

with $m_p,m_T$ the projectile and target atomic mass, respectively, and $E_0$ the projectile initial kinetic energy in the laboratory system. Introducing Eq. (24) into Eq. (2) the inelastic energy loss from a given atomic orbital $\lambda$, with population $\omega_\lambda$, of either projectile or target reads as

$$\epsilon_\lambda(b,E_0)=\tfrac{1}{4}m\mu_0\omega_\lambda\langle v_\lambda\rangle\int_{R_0}^{\infty}\frac{[1-V(R)/E_{\rm rel}]dR}{[1-V(R)/E_{\rm rel}-b^2/R^2]^{1/2}}\int\psi_\lambda^*\psi_\lambda dA\ , \tag{26}$$

with $R_0$ the distance of closest approach in the collision evaluated through the condition

$$1-V(R)/E_{\rm rel}-b^2/R_0^2=0\ . \tag{27}$$

Following Latta and Scanlon[21] we may remove the singularity in the integral over $R$ in Eq. (26) by adopting the variable $\kappa$ where

$$\kappa=(1-R_0/R)^{1/2}\ . \tag{28}$$

Introducing the HFS wave functions [Eq. (12)] and after integrating over the Firsov plane, Eq. (26) reduces to

$$\epsilon_\lambda(b,E_0)=(1/2b)mv_0R_0^2\omega_\lambda\langle v_\lambda\rangle\int_0^1\frac{1-V(R_0/(1-\kappa^2))E_{\rm rel}^{-1}(1-\kappa^2)^{-2}d\kappa\,\mathcal{S}(\nu,\eta,\alpha)}{\left[2-\kappa^2+\frac{R_0^2}{b^2\kappa^2E_{\rm rel}}[V(R_0)-V(R_0/(1-\kappa^2))\right]^{1/2}}\,, \tag{29a}$$

with

$$\mathcal{S}(\nu,\eta,\alpha)=\sum_{p,q}C_pC_q\exp[-\eta\alpha R_0/(1-\kappa^2)]\sum_{s=0}^{\nu-1}\frac{(\nu-1)!}{s!}\left[\frac{\alpha R_0}{1-\kappa^2}\right]^s\eta^{s-n_p-n_q}\,, \tag{29b}$$

where $v,\eta$ are given by Eq. (15) and $\alpha$ denotes, as before, the fractional position of the distance between projectile and target where the Firsov plane is located.

The total inelastic loss due to projectile and target is thus the sum over all occupied orbitals of both systems, i.e.,

$$\epsilon(b,E_0)=\left[\sum_\lambda\epsilon_\lambda\right]_p+\left[\sum_{\lambda'}\epsilon_{\lambda'}\right]_t \tag{30}$$

(where $p$ represents projectile and $t$ represents target) and the electronic-stopping cross section may then be evaluated through Eq. (3).

Equations (29a) and (29b) should be regarded as the most general expression to obtain the inelastic energy loss in a collision within the Firsov model and, from this moment, they will constitute our working equations in order to proceed with our analysis. We first note that the quantity $\epsilon(b,E_0)$ is dependent on the kind of interatomic potential used to describe the binary interaction and also dependent on the position of the Firsov plane. It is therefore pertinent to analyze how sensitive it is to the different choice of these quantities, since this will have direct consequences in the evaluation of $S_e$.

TABLE II. Average and rms speeds for some atoms and ions.[a]

| System | Orbital | $\langle v\rangle$ | $v_{\rm rms}$ |
|---|---|---|---|
| H | 1s | 0.849 | 1.000 |
| Ar | 1s | 14.789 | 17.554 |
| | 2s | 3.942 | 7.085 |
| | 3s | 1.026 | 2.762 |
| | 2p | 6.155 | 6.919 |
| | 3p | 1.713 | 2.395 |
| $Li^+$ | 1s | 2.249 | 2.690 |
| $Na^+$ | 1s | 8.319 | 10.609 |
| | 2s | 2.241 | 3.699 |
| | 2p | 2.976 | 3.437 |

[a]All quantities in units of bohrs.

### 1. Sensitivity to the interatomic potential

Evidently, the quantity of central importance in any trajectory calculation is the pairwise interaction potential. In the past, the most commonly used potentials have been of the Bohr[22] or Thomas-Fermi type[23] or some improved version of them.[24] However, it is worth pointing out that while the Thomas-Fermi potential overestimates the interaction for relatively large separations, the Bohr potential underestimates it, and in a way we should consider these as two extreme cases, as pointed out by Kalbitzer *et al.*[25] Only recently has attention been paid to more elaborate and realistic descriptions of the repulsive potential based either on *ab initio* SCF (self-consistent-field) calculations[26–28] or on approximations made through density-functional approaches employing the HFS atomic orbitals.[29–31] To analyze the sensitivity of the trajectory calculation to the type of interatomic potential we shall evaluate $\epsilon(b,E_0)$ using the Bohr, Thomas-Fermi-Molière (TFM), and realistic potentials, respectively. The Thomas-Fermi-Molière potential is given by

$$V_{\rm TFM}(R)=(Z_1Z_2e^2/R)\chi_{\rm TFM}(R/a)\,, \tag{31}$$

where, as usual, $Z_1$ and $Z_2$ represent the atomic number of projectile and target, respectively, and $\chi(R/a)$ is the Molière screening function[24]:

$$\chi_{\rm TFM}(R/a)=0.35e^{-0.3R/a}+0.55e^{-1.2R/a}+0.10e^{-6R/a}\,, \tag{32}$$

where $a$ is the Thomas-Fermi screening length:

$$a=0.8853a_0(Z_1^{2/3}+Z_2^{2/3})^{-1/2}\,. \tag{33}$$

For the Bohr potential we shall use the expression

$$V_B(R)=(Z_1Z_2e^2/R)e^{-0.8853R/a}\,. \tag{34}$$

Finally, for the realistic potential we shall use the results of either *ab initio* calculations or the near-*ab initio* quality calculations of Gordon and Kim[29] which are based on the statistical model of the atom but employing HFS wave functions to describe the electronic density of the atom, following the perturbative approach first made by Lenz and Jensen.[32,33] Although these potentials do not have an analytical

TABLE III. Average and rms speeds for selected orbitals in Cu(3S) for different basis sets.[a]

| Orbital | Minimal | Single $Z$ | Double $Z$ | Extended |
|---|---|---|---|---|
| 3s | 2.017 | 1.042 | 0.959 | 1.662 |
| | (2.325) | (5.918) | (5.721) | (5.731) |
| 3p | 3.133 | 3.328 | 3.711 | 3.799 |
| | (3.354) | (5.281) | (5.392) | (5.403) |
| 3d | 4.098 | 3.913 | 3.771 | 3.726 |
| | (4.400) | (4.202) | (4.342) | (4.338) |
| 4s | 0.472 | 0.380 | 0.535 | 0.589 |
| | (0.552) | (0.718) | (1.081) | (1.185) |

[a]Values in parentheses are for $v_{\rm rms}$. All quantities in units of bohrs.

expression, it has been shown recently[27] that they can be properly parametrized into the screened Coulomb plus Born-Mayer expression:

$$V(R)=(Z_1Z_2e^2/R)(ARe^{-\alpha R}+e^{-\beta R}) , \quad (35)$$

where the quantities $A,\alpha,\beta$ are parameters obtained through a least-squares fit to the numerical values. In Figs. 4(a), 4(b), and 4(c) we show the potential energy curves according to the different descriptions discussed above for some particular examples. As is apparent from these figures the parametrization given by Eq. (35) describes reasonably well the realistic potential (less than 10% difference on the average) for a relatively wide range of internuclear separations.

To investigate the sensitivity of $\epsilon$ to the inclusion of a trajectory calculation as well as to the choice of interatomic potential, we have first kept the position of the Firsov plane fixed half-way between projectile and target ($\alpha=0.5$ in Eq. (29)] and evaluate the inelastic energy loss as a function of the impact parameter through Eqs. (31)–(36) for the different interatomic potentials and energies. Figures 5(a) and 5(b) show the results of this calculation for $Li^+$-Ne and $Na^+$-Ne, as an example. As the reader must be aware from this figure, the importance of the nonrectilinear trajectory calculation becomes evident for very low energies ($\lesssim 2$ keV) and very large differences ($\sim 500\%$) are detected between the evaluation of $\epsilon$ with this approach compared to that using a rectilinear trajectory approximation [$V=0$ in Eq. (29)]. Furthermore, the sensitivity of $\epsilon$ to the particular type of potential becomes higher as the energy is reduced and, as expected, the long- (short-) range character of the Molière (Bohr) potential is reflected by the slow (fast) convergence of the corresponding curve to the $V=0$ case. Interestingly enough, the rectilinear trajectory approximation turns out to be very good for energies higher than about 10 keV for all practical purposes, as was verified also for other cases. This fact justifies widely the use of a rectilinear trajectory approximation in order to describe the inelastic energy loss, within this model, in gas or solid-thin-film transmission experiments. For range studies, however, we should be aware of the increasing importance of the trajectory and thus accurate interatomic potentials should be used as slowing down takes place in order to properly account for the inelastic energy losses, as pointed out by Wilson *et al.*[34] for the case of nuclear stopping.

### 2. *Sensitivity to the position of Firsov's plane*

So far all the calculations have been done keeping the Firsov plane at the half-way position, regardless of the type of systems involved in the collision. By these means the importance of the interatomic potential was indicated and the validity of the rectilinear trajectory approximation confirmed for energies above $\sim 10$ keV. Let us now study quantitatively the importance of the location of the plane in the calculations. To do this, a particular interatomic potential has been selected; in this case, the Molière potential; and different estimates for the position of the plane have been used in the calculations.

For any interatomic distance, $\alpha$ corresponds to the fractional position between the colliding partners where the atomic potential is the same for the electrons of projectile and target. This will define the region of "influence" of each of the systems, dividing the space into the two physical regions necessary in the flux calculation.

Rather than using an approximate analytical atomic potential, like that proposed by Green *et al.*,[35] for example, we shall use the HFS wave function given by Eq. (12) to construct the electronic density and solve Poisson's equation to obtain the atomic Hartree-Fock potential. Next, the parameters $\alpha$ and $\alpha'=1-\alpha$, which define the distance from

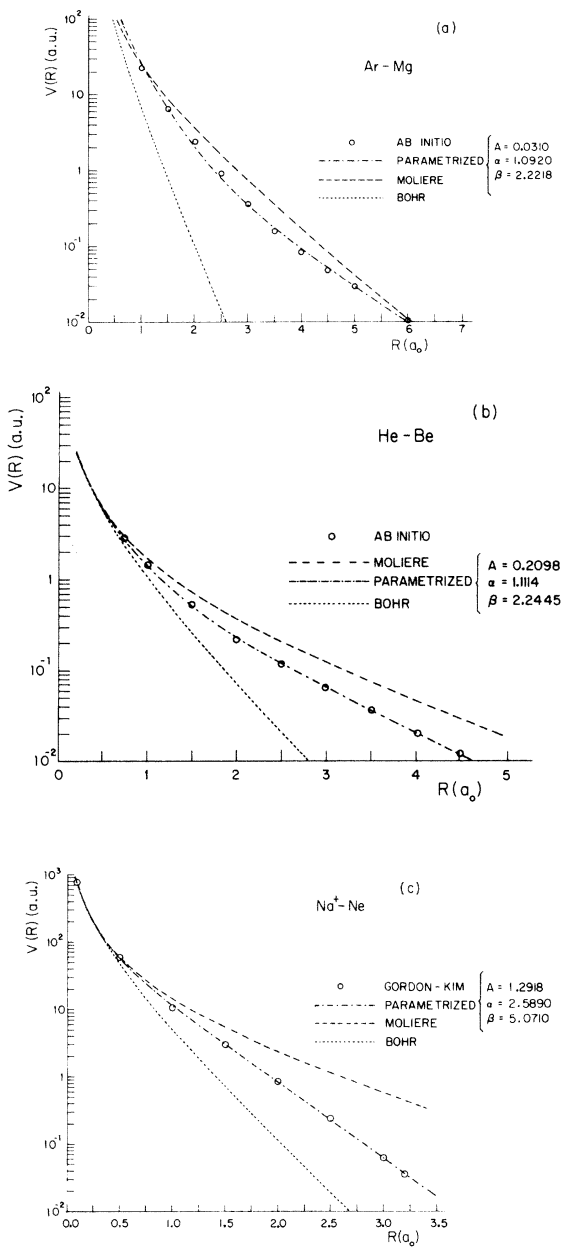


FIG. 4. Bohr, Thomas-Fermi-Molière, and realistic interaction potentials in the repulsive region for some cases: (a) Ar-Mg *ab initio* (Ref. 28), (b) He-Be *ab initio* (Ref. 27), (c) $Na^+$-Ne from Ref. 29(a). The parameters $A$, $\alpha$, and $\beta$ correspond to the best fit of Eq. (35) to the numerical values (see text).

the plane to target and projectile, respectively, are obtained.

With the aid of Eq. (12) and after solving Poisson's equation for the radial charge density it may be proven that the electrostatic potential due to orbital $\lambda$ is

$$W_\lambda(r)=-\sum_{p,q} C_p C_q \frac{\nu!}{\eta^{\nu+1} r} e^{-\eta r} \mathscr{Y}_{p,q} , \tag{36}$$

where

$$\mathscr{Y}_{p,q}=1+\sum_{k-2}^{\nu} \frac{(k-2)!}{k!} \sum_{\tau=0}^{k-2} \frac{(\eta r)^{\tau+1}}{\tau!} , \tag{37}$$

and $\eta,\nu$ are as defined in Eq. (15). The total electrostatic potential at the distance $r$ from the nucleus is then due to the superposition of all orbitals, i.e.,

$$W(r)=\sum_{\lambda} \omega_\lambda W_\lambda(r) , \tag{38}$$

with $\omega_\lambda$ the population of orbital $\lambda$. The fractional position at which Firsov's plane is located between projectile and target is then obtained at the point where

$$W_p(r)=W_t(r)(\,|R-r|\,) , \tag{39a}$$

where the indices $p$ and $t$ stand for projectile and target, respectively and $R$ is the relative distance.

Note the implicit dependence of $\alpha$ on the integration variables in Eq. (29a). We are then bound to evaluate $\alpha$ through Eq. (39a) for each integration point along the trajectory. This amounts to consider the Firsov plane as moving, as projectile and target move relatively to each other. Since this calculation becomes too time consuming, we decided to see whether the motion of the plane was important or not. For this purpose we calculated an average value for $\alpha$ obtained as

$$\langle \alpha_{\rm HFS} \rangle = \frac{1}{r_m - r_0} \int_{r_0}^{r_m} \alpha(r) dr , \tag{39b}$$

where $\alpha(r)$ is a minimax polynomial approximation[36] to the numerically calculated $\alpha$ values as a function of distance in the range $0.01a_0 \le r \le 8a_0$.

No appreciable differences were observed in the values of $\epsilon(\alpha b)$ when the constant average value $\langle \alpha_{\rm HFS} \rangle$ was employed instead of the full calculation, as may be verified from Figs. 6(a) and 6(b). This result indicates that the motion of the Firsov plane is not relevant in this approach. Figures 6(a) and 6(b) also show the values obtained through the use of the half-way plane criterion[1] and the criterion proposed by Kishenevsky,[37] which considers the fractional position $\alpha_p$ measured from the heavier collision partner as

$$\alpha_p=[1+(Z_L/Z_H)^{1/6}]^{-1} , \tag{40}$$

where $Z_H$ ($Z_L$) is the atomic number of the heavy (light) system.

Observe, for the particular cases shown in those figures, how important the location of the plane becomes. In general, the criterion given by Eq. (40) gives a good average description for the whole range

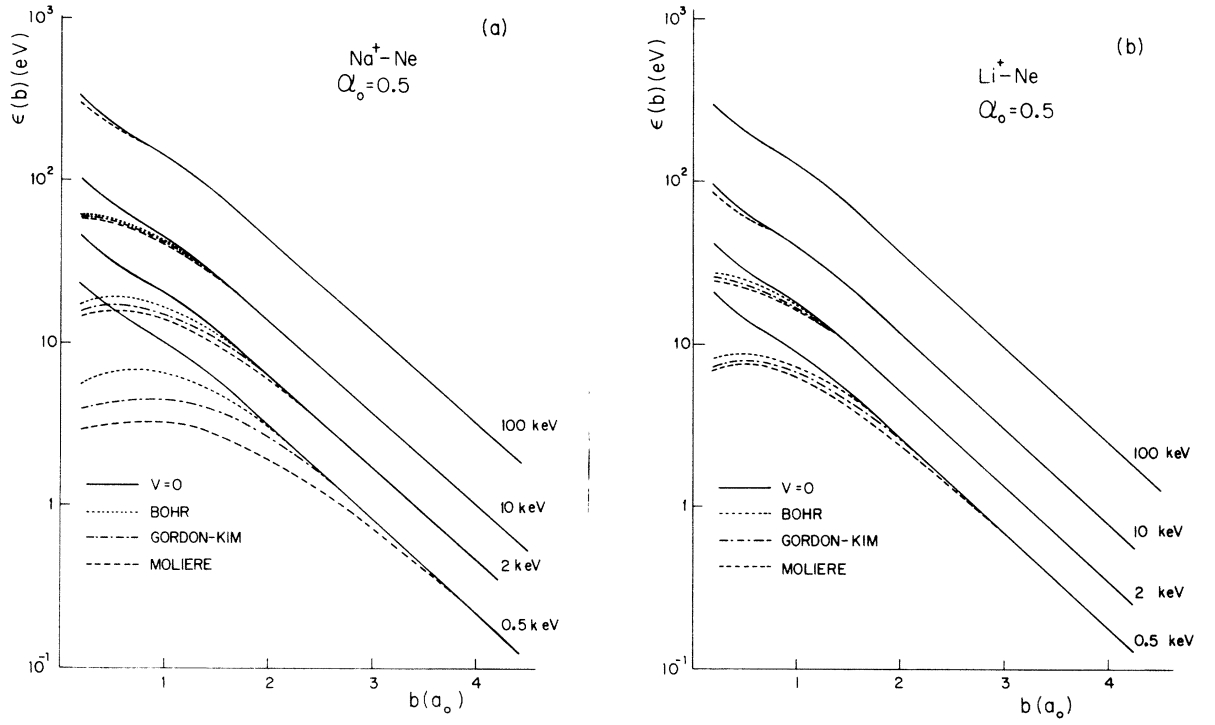


FIG. 5. Inelastic energy loss as a function of impact parameter [Eq. (29)] for different interatomic potentials and energies for (a) $Na^+$-Ne and (b) $Li^+$-Ne, respectively. In both cases the Firsov plane has been kept half-way between projectile and target.

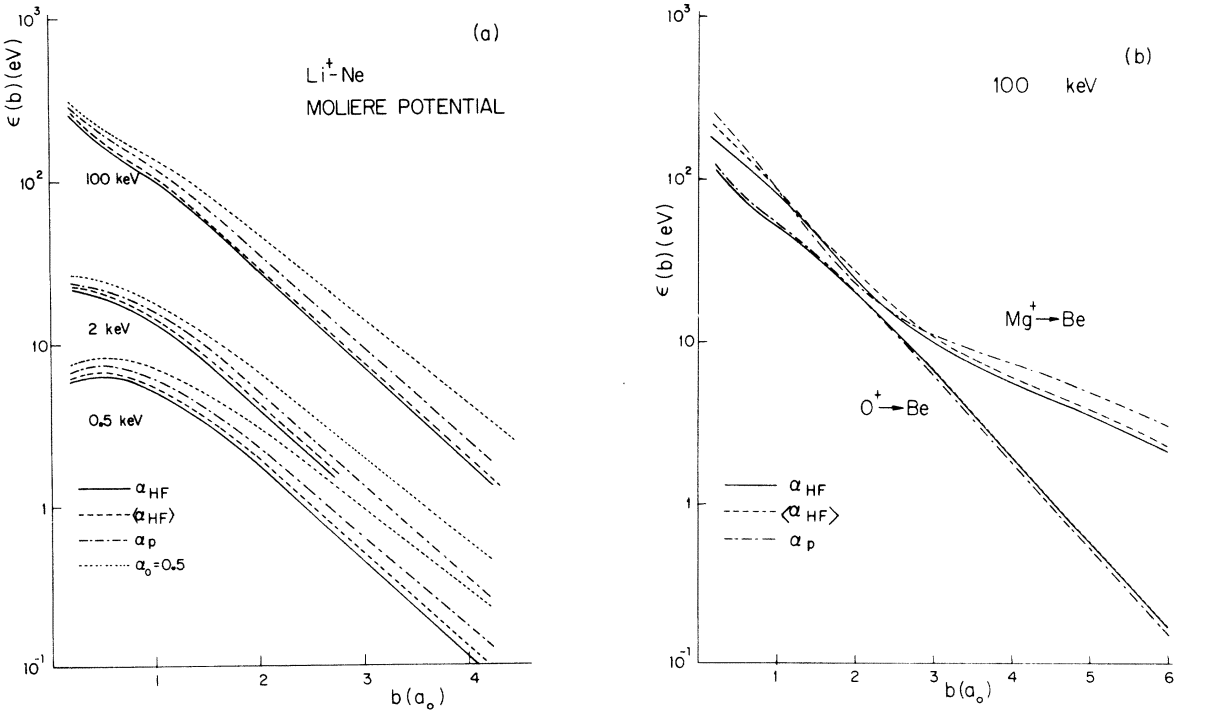


FIG. 6. Inelastic energy loss as a function of impact parameter [Eq. (29)] for different estimates of the position of the Firsov plane. The Molière potential was used in the trajectory calculation. (a) $Li^+$-Ne for various energies, (b) 100 keV $Mg^+$-Be and $O^+ \rightarrow$Be, the curve for $\alpha_0 = 0.5$ has been omitted in this last figure for clarity.

of interest (up to about 20% difference with the values obtained with $\alpha=0.5$ or $\langle\alpha_{\rm HFS}\rangle$) and, interestingly, the relative differences among the various approaches appear to be independent of projectile energy. Since the position of the plane is of such relevance in the calculations we have estimated the differences in its location when the projectile is either a singly charged positive ion or a neutral atom. Table IV shows the average parameters $\langle\alpha_{\rm HFS}\rangle$ for both neutral and singly positive charged projectiles along with the corresponding estimates from Eq. (40). We note first that there are considerable differences ($\pm 10\%$) in the location of the plane when the different charge states for the projectile are used. On the other hand, the Kishenevsky criterion [Eq. (40)] gives, in general, a reasonable estimate for the position of the plane. This criterion will therefore be used in the forthcoming analysis.

Note that the $\epsilon$ curves for $Li^+$-Ne,$Mg^+$-Ne, $O^+$-Be in Figs. 6(a) and 6(b) exhibit, in general, an exponential behavior for relatively large values of impact parameter (and, therefore, of distances of closest approach) as first pointed out by Oen and Robinson.[38] However, the inclusion of shell structure in these calculations is apparent in Fig. 6(b), for example, where the extended $3s$ orbital of $Mg^+$ seems to be responsible for the still high contribution to $\epsilon$ even for relatively large values of $b$. This trend is also observed in other colliding pairs and has been previously pointed out by several authors.[11,39]

TABLE IV. Values for $\langle\alpha_{\rm HFS}\rangle$ and $\alpha_p$ for several projectile target combinations.

| Projectile | Target | $\langle\alpha_{\rm HFS}\rangle$[a] | $\alpha_p$ |
|---|---|---|---|
| $Be^+$ | C | 0.54 (0.47) | 0.52 |
| $Ne^+$ | C | 0.41 (0.44) | 0.52 |
| $Ti^+$ | C | 0.56 (0.51) | 0.55 |
| $C^+$ | Ne | 0.49 (0.45) | 0.52 |
| $Mg^+$ | Ne | 0.57 (0.62) | 0.51 |
| $O^+$ | He | 0.54 (0.60) | 0.56 |
| $O^+$ | O | 0.45 (0.50) | 0.50 |
| $Cu^+$ | Cu | 0.39 (0.50) | 0.50 |

[a]Values in parentheses correspond to neutral projectiles.

## IV. COMPARISON WITH EXPERIMENT

So far, we have found the importance of the various quantities that enter the calculation of the inelastic energy loss (and, therefore, of $S_e$) within Cheshire's modification to the Firsov model. We shall now apply the theory (without any fitting parameters) to evaluate the electronic-stopping cross section for several cases and compare it with the experimental measurements reported in the literature. This will provide information relevant to the scope of the Firsov model as modified by Cheshire, when all the quantities involved in the calculation are evaluated consistently.

In all the calculations we shall use the extended HFS atomic wave functions together with the average speed for the atomic electrons as well as the rectilinear trajectory approximation. For this purpose we have chosen the data from transmission experiments through gaseous targets as well as thin solid films ($\sim$400-Å thickness). In order to be able to compare the predictions of the Firsov model with experimental measurements it is necessary to relate the macroscopic experimental variables (i.e., target thickness, gas pressure, detector solid angle, etc.) to the average properties of the individual collision events. In particular, multiple scattering often causes a portion of the transmitted beam to lie outside the detector acceptance angle. The experiment thus measures $S_e$ only for a selected subpopulation of the transmitted particles. We take this effect into account here by evaluating a minimum impact parameter $b_0$, which is consistent with the experimental geometry, i.e., particles which have collisions with impact parameter less than $b_0$ suffer large-angle deflections and are thus not counted.

Although the experimental measurements considered here all involve "thin" targets (i.e., $\sim$400 Å for the solid targets, and equivalent thickness for the gaseous targets), they are not sufficiently thin that correlation effects are important.[40] Thus, we may make a straightforward statistical analysis of the multiple scattering suffered by the beam.

Let the root-mean-square scattering angle for the individual small-angle collisions be defined as $\theta_{\rm rms}$ where

$$\theta_{\rm rms}^2 \equiv \int_0^{\theta_0} \theta^2\sigma(\theta)\sin\theta\, d\theta \Big/ \int_0^{\theta_0} \sigma(\theta)\sin\theta\, d\theta \ , \tag{41}$$

with $\theta_0(b_0)$ a maximum scattering angle consistent with the minimum impact parameter $b_0$.

In Eq. (41) $\sigma(\theta)$ is the differential cross section for scattering into the solid angle $\sin\theta\, d\theta$. Let $\theta_L(x)$ be the root-mean-square angular deflection of a particle beam transmitted through a target of thickness $x$. Then $\theta_L$ is related to $\theta_{\rm rms}$ through the equation

$$\frac{d}{dx}\theta_L^2 \equiv n\int_0^{\theta_0}\theta^2\sigma(\theta)\sin\theta\, d\theta = n\theta_{\rm rms}^2\sigma_0 , \quad (42a)$$

where $n$ is the target atomic density and $\sigma_0$, given by

$$\sigma_0 = \int_0^{\theta_0}\sigma(\theta)\sin\theta\, d\theta , \quad (42b)$$

is the total small-angle scattering cross section.

Equation (42a) is readily integrated for thin targets (i.e., assuming that $\Delta E$ is small so that $\sigma_0$ is not a function of depth) to yield

$$\theta_L^2 = n\sigma_0 x\theta_{\rm rms}^2 . \quad (43)$$

If one identifies $\theta_L$ with the detector acceptance angle then, Eqs. (41)—(43) can be used to determine a value of $\theta_0$. This is equivalent to fixing a minimum impact parameter for the experimentally observed subpopulation of transmitted projectiles.

Following the idea of near rectilinear trajectories and using the impulse approximation for a binary collision, it may also be shown[41] that

$$E_0\theta_{\rm rms} = b_0\int_{b_0}^{\infty}\left[-\frac{\partial V}{\partial R}\right](R^2-b_0^2)^{-1/2}dR , \quad (44)$$

where $V(R)$ is the interatomic potential and $E_0$ and $\theta_{\rm rms}$ are the projectile energy and individual scattering angle in the laboratory, respectively.

Equations (41)—(44) provide us with a useful means to calculate the minimum impact parameter necessary in the calculations of $S_e$ [cf. Eq. (3)], consistent with the appropriate experimental conditions. Dependence of the minimum impact parameter on interatomic potential is also accounted for in the near rectilinear trajectory approximation through Eq. (44).

For thin amorphous and polycrystalline targets we have considered the scattering cross section as[42]

$$\sigma_s = \pi\tau^2, \quad \tau \approx 0.5n^{-1/3} , \quad (45)$$

where $t$ is the mean interatomic distance. For gaseous targets we used

$$\sigma_g = \pi b_0^2 , \quad (46)$$

with $b_0$ the impact parameter, which in this case is obtained self-consistently when Eq. (46) is inserted into Eq. (44) (see below).

After little manipulation with the help of Eqs. (43)—(46), it may be shown that

$$(1.128)d^{-1/2}n^{-1/6}E_0\theta_L^s = Z_1Z_2e^2f(b_0) , \quad (47)$$

$$(k_BT/P\pi d)^{1/2}E_0\theta_L^g = Z_1Z_2e^2b_0f(b_0) , \quad (48)$$

where $s$ and $g$ stand for solid and gas targets, respectively. $k_B$ is Boltzmann's constant, $T$ the absolute temperature, $P$ the pressure in the gas target chamber, $d$ the target thickness, and $f(b_0)$ a function of $b_0$ obtained after integration of the particular interatomic potential used in Eq. (44). For the Bohr, Molière, and parametrized potentials [see Eqs. (31)—(35)], we obtain, for $f(b_0)$,

$$0.8853a^{-1}K_1(0.8853b_0/a)\ \text{(Bohr)} , \quad (49)$$

$$a^{-1}[0.35K_1(0.3b_0/a)+0.55K_1(1.2b_0/a)+0.1K_1(6b_0/a)]\ \text{(Molière)} , \quad (50)$$

$$\alpha Ab_0K_0(\alpha b_0)+\beta K_1(\beta b_0)\ \text{(parametrized)} , \quad (51)$$

where $K_0$ and $K_1$ are the zeroth- and first-order modified Bessel functions of the first kind,[43] respectively. Equations (47) and (48) were solved numerically for $b_0$ for the three potentials mentioned above. Table V shows the results for some particular examples. Note that the Bohr potential gives quite reasonable estimates for $b_0$ as compared to those from the realistic potential, whereas the Molière potential gives systematically higher values of $b_0$ which is to be expected due to its long-range character. In view of its simplicity and the fact that it gives calculated $b_0$ values in reasonable agreement with those obtained using more sophisticated potentials, the Bohr potential has been used in the following calculations. The use of the Bohr potential in this case is, on the other hand, consistent with the requirement of a short-range interaction in order to consider uncorrelated events in the treatment of the collision sequence, mainly in solids.

In the light of the previous analysis we have calculated $S_e$ for several cases shown in Figs. 7—11. In all the cases shown the corresponding values for $b_0$ were obtained according to Eqs. (47) and (48). Fig-

TABLE V. Some values of $b_0$ obtained for different potentials according to Eqs. (47)—(51) for solid and gas targets.[a,b]

| System | Bohr | Molière | Realistic |
|---|---|---|---|
| $Li^+$-Ne | 1.24 | 3.87 | 1.55[c] |
| $Na^+$-Ne | 1.08 | 3.36 | 1.56[c] |
| He-Be | 1.40 | 3.10 | 1.61[d] |
| Ar-Mg | 1.15 | 2.70 | 1.70[e] |
| Mg-Ne | 1.08 | 3.36 | 1.48[e] |

[a]All values in a.u.

[b]Projectile velocity $v = 0.9v_0$. For solid targets a thickness of 300 Å is assumed. For gas targets $P = 0.1$ torr, $T = 273$ K, $d = 0.8m$. In all cases the half detection angle is $\Theta_L = 0.165°$.

[c]Potential from Ref. 29.

[d]Potential from Ref. 27.

[e]Potential from Ref. 28.

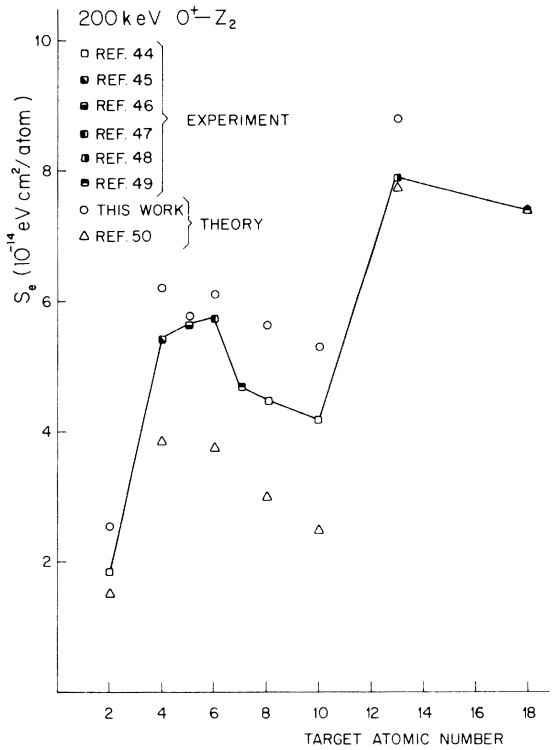


FIG. 7. Experimental measurements and theoretical estimates for 200-keV oxygen ions incident on several targets.

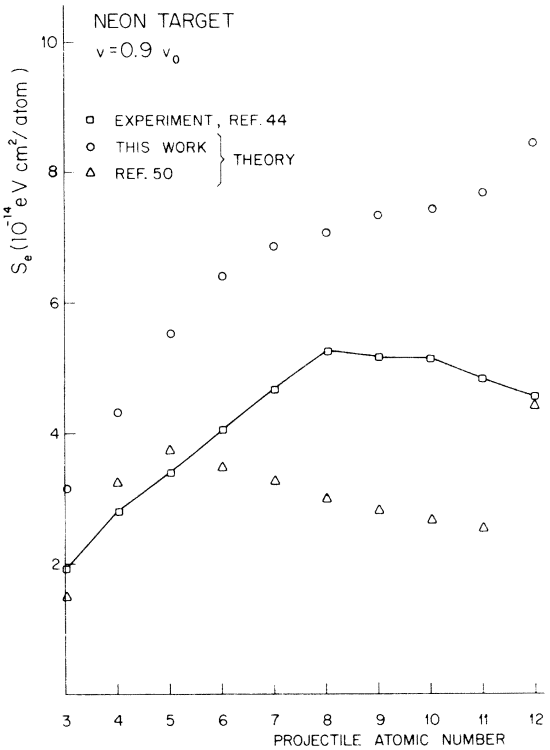


FIG. 8. Theoretical estimates and experimental measurements of the electronic-stopping cross section for several projectiles ($v = 0.9v_0$) incident on neon.

ure 7 displays the results for 200-kev oxygen ions incident on various targets ($2 \leq Z \leq 18$) along with the experimental data and conditions taken from the literature.[44–49] For beryllium targets, the experimental value for $S_e$ was obtained from range measurements[45] and therefore we used the value $b_0 = 0$ in the equation for $S_e$ to get an estimate, assuming that the rectilinear trajectory approximation is still reasonable for most of the individual collision events, where the inelastic losses are still dominant. For nitrogen and argon targets no theoretical estimate was made due to the lack of information on the experimental conditions.[49] Apart from the relatively good quantitative agreement between theory and experiment in this case, we note that the amplitude of the oscillations in $S_e$ is well described when proper distinction is made between solid and gas targets through Eqs. (47) and (48). Also shown are the theoretical predictions of Land *et al.*[50] who used the rectilinear trajectory approximation, together with the extended basis set, rms speed, and a fixed value for $b_0$ ($=2.5$ a.u.) for all the cases.

Figure 8 shows the theoretical estimates and experimental measurements[44] for several projectiles ($3 \leq Z \leq 12$) with velocity $v = 0.9v_0$ incident on neon. Our calculations lie systematically high with respect to experiment. This may be partly due to the fact that $b_0$ was evaluated using the Bohr potential, the short-range character of which makes it less suitable than the realistic potential for describing ion-gas collisions at the energies considered, as shown in Table V for the neon target. This figure shows also the results of Land *et al.* as a comparison.

In Fig. 9 we show the experimental measurements of $S_e$ in thin carbon films for several projectiles with velocities $v = 0.41v_0$,[47,48] and $v = 0.63v_0$ (Ref. 51) along with our theoretical predictions and those from Ref. (50). Although some of the experimentally observed trends are reasonably well described by the theory, the agreement with experiment is similar to that obtained by Land and Brennan[50] using fitting parameters. There are a number of features which are clearly not explainable in terms of the Firsov model. For the $v = 0.41v_0$ case, the overall qualitative agreement appears to be better than that obtained for the higher velocity but the quantitative agreement, particularly for projectiles from neon to phosphorous where differences between theory and

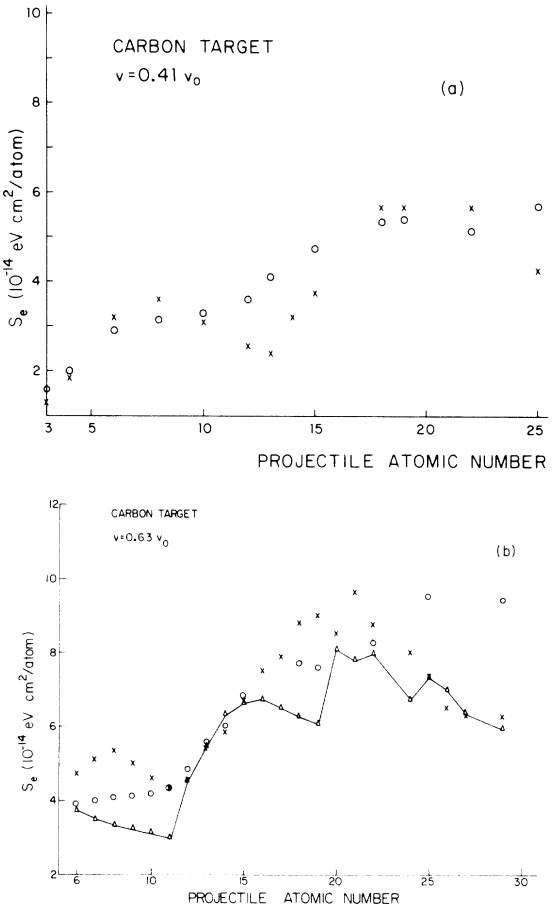


FIG. 9. Theoretical estimates and experimental measurements of the electronic-stopping cross section for several projectiles incident on carbon targets. (a) $v=0.41v_0$; (b) $v=0.63v_0$; ○, theory, this work; △, theory from Ref. 50; ×, experiment (Refs. 51 and 52).

experiment are as high as 60%, is significantly worse. The results at the higher velocity for the transition elements shown ($21 \leq Z \leq 30$), while still consistently high, represent a considerable improvement over our previous calculations.[7] This is not unexpected since the extent of the $3d$ and $4s$ orbitals, which make the most important contribution to $S_e$,[14] necessitate a larger value of $b_0$ than the fixed 1 a.u. used in the earlier calculations.

Figure 10 displays the corresponding theoretical results as well as experimental data[48] for various projectiles incident on an aluminium target ($v=0.41v_0$). Here, there is good overall quantitative agreement, although the shape is not too well reproduced.

Finally, Fig. 11 shows the results of this calculation for singly stripped ions ($v=0.68v_0$) channeled in the ⟨110⟩ direction of a silicon single crystal along with experimental data.[52] In this case $b_0$ was

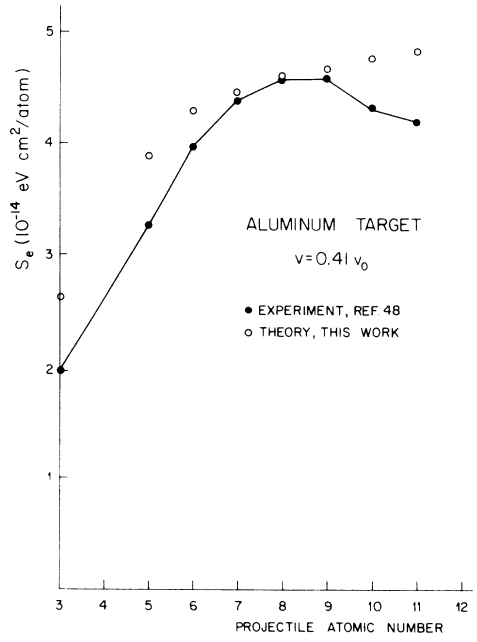


FIG. 10. Electronic-stopping cross-section measurements and theoretical predictions for several ions ($v=0.41v_0$) incident on aluminium.

set equal to the channel halfwidth ($b_0=3.82$ a.u.) and $\epsilon$ summed over the number of collisions per unit path length. The positions of the oscillations are qualitatively well predicted, but clearly the magnitude of $S_e$ is overestimated. One probable reason for this is that the charge density within the channel is much smaller than implied by the use of free-atom charge distributions. This directional effect is not present in amorphous materials where, on the average, we could superimpose free-atom charge distri-

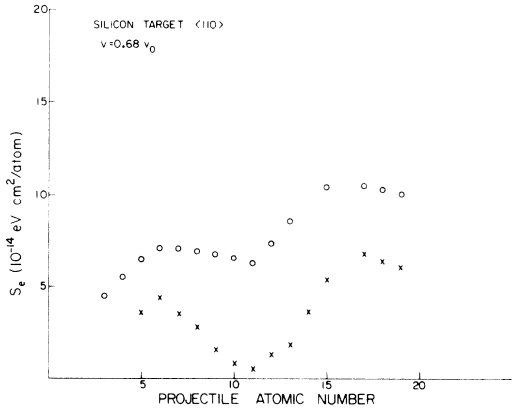


FIG. 11. Experimental measurements and theoretical predictions for several projectiles ($v=0.68v_0$) channeled along the ⟨110⟩ direction of a silicon single crystal. ×, experiment (Ref. 53); ○, theory, this work.

butions to account for the total charge density in the material.

## V. CONCLUSIONS

We have made an exhaustive analysis of all factors that could affect the predictions of the inelastic energy loss within the Firsov model as modified by Cheshire. Our findings can be summarized as follows.

(1) The results of calculations using this model are highly sensitive to the choice of the wave function and the speed of the atomic electrons. It is suggested, for the sake of consistency, that accurate wave functions and the average speed should be used in any calculations within the model.

(2) The nonrectilinear trajectory calculation was found to be relevant only for very low energies ( $\lesssim 10$ keV) and therefore the use of the rectilinear trajectory approximation is justified for projectile energies higher than about 10 keV in the description of transmission experiments. For the analysis of range measurements the full trajectory calculation should be used together with a realistic potential due to the large differences ( $\sim 500\%$) observed when the projectile energy becomes very low.

(3) We have given quantitative support to the Kishenevsky criterion for the location of Firsov's plane and found that the motion of this hypothetical plane is negligible for all practical purposes.

(4) To evaluate univocally the minimum impact parameter involved in the calculations it is necessary to take proper account of the experimental conditions (target thickness, detection angle, gas chamber pressure, etc.), and to utilize the appropriate interatomic potential.

We have shown explicitly the role of the different quantities that enter the calculations which should be considered if any adjustable parameter is to be used in this model. Overall, we find that using the most accurate wave functions available, a proper average speed, a minimum impact parameter based on reasonable interatomic potentials, and locating the Firsov plane at the saddle point of the total potential seen by the electrons, the Firsov theory is accurate only to within a factor of 2. However, the *relative* values of $dE/dx$ as functions of either $Z_1$ (projectile atomic number) or $Z_2$ (target atomic number) are reasonably well reproduced by the theory ( $\sim 10\%$). We, therefore, conclude that the Firsov theory may be used with confidence to obtain $dE/dx$ for a given projectile target $(Z_1,Z_2)$ combination provided experimental data are available for nearby values of $(Z_1,Z_2)$ in order to evaluate the scale factor. The Firsov theory may also be useful in comparing results for different $(Z_1,Z_2)$ combinations when only relative effects are important.

## ACKNOWLEDGMENTS

One of us (S.A.C.) would like to express his deep gratitude of the Group of Atomic Collision in Solids of the University of Salford, especially George Carter, Mike Nobes, and Dave Armour, for giving him the opportunity to collaborate in many interesting problems during his sabbatical leave and for all the fruitful and illuminating discussions. This work was partially supported by the International Atomic Energy Agency under Contract No. 2729/RB. One of us (E.V.A.) was a recipient of a fellowship from the Consejo Nacional de Investigaciones Científicas y Técnicas de la República Argentina. A portion of the work of D.K.B. was performed at Sandia National Laboratories, supported by the U. S. Department of Energy under Contract No. DE-AC04-76DP00789.

## APPENDIX

In this appendix we show the main steps followed to obtain the expression for $\langle v_\lambda \rangle$ given in Eq. (21). The average electron speed of orbital $\lambda$ is given (in units of $v_0=\hbar/ma_0$) as

$$\langle v_\lambda \rangle = 4\pi \int_0^\infty \Phi_\lambda^*(k) k^3 \Phi_\lambda(k) dk \ , \tag{A1}$$

where $\Phi_\lambda(k)$ is the radial part of the Fourier transform given by Eq. (20). After substitution of this last equation into Eq. (A1) it may be shown that, for terms with $p \neq q$,

$$\langle v_\lambda \rangle_{p\neq q} = 2^{2\lambda+3}(\lambda!)^2 \sum_{p,q} C_p C_q (-1)^{n_p+n_q} D^{n_p-\lambda,n_q-\lambda} \int_0^\infty \frac{k^{2\lambda+3} dk}{(k^2+\xi_p^2)^{\lambda+2}(k^2+\xi_q^2)^{\lambda+1}} \ , \tag{A2}$$

where the differentiation operator $D^{a,b}$ is defined as

$$D^{a,b} = \frac{\partial^a}{\partial \xi_p^a} \frac{\partial^b}{\partial \xi_q^b} \ . \tag{A3}$$

Introducing the new variable, $u = 1/k^2$, Eq. (A2) may be expressed more suitably as

$$\langle k_\lambda \rangle_{p\neq q} = 2^{2\lambda+3}(\lambda!)^2(\lambda+1)\sum_{p,q} C_p C_q (-1)^{n_p+n_q+1} D^{n_p-\lambda-1,n_q-\lambda}[\xi_p I(\lambda,\lambda+2,\lambda+1;\xi_p^2,\xi_q^2)] , \tag{A4}$$

where

$$I(\lambda,\lambda+2,\lambda+1;\xi_p^2,\xi_q^2) = \int_0^\infty \frac{u^\lambda du}{(1+\xi_p^2 u)^{\lambda+2}(1+\xi_q^2 u)^{\lambda+1}} . \tag{A5}$$

The integrals appearing in Eq. (A5) have been obtained explicitly in Ref. 14 and therefore we do not write them here for the sake of space. We note now that, since $n_p, n_q > \lambda$, then

$$D^{n_p-\lambda-1,n_q-\lambda}(\xi_p) = 0 , \tag{A6}$$

and therefore Eq. (A4) becomes finally as

$$\langle k_\lambda \rangle_{p\neq q} = 2^{2\lambda+3}(\lambda!)^2(\lambda+1)\sum_{p,q} C_p C_q (-1)^{n_p+n_q+1} \xi_p D^{n_p-\lambda-1,n_q-\lambda} I(\lambda,\lambda+2,\lambda+1;\xi_p^2,\xi_q^2) . \tag{A7}$$

For terms with $p = q$, it may easily be shown that

$$\langle k_\lambda \rangle_{p=q} = 4\sum_p C_p^2 \sum_{g,h} K(n_p,g,h;\lambda)\xi_p^{-2n_p}(\lambda+1)! , \tag{A8}$$

where

$$K(n_p,g,h;\lambda) = \frac{(-1)^{g+h}[(n_p-\lambda)!]^2(n_p-g)!(n_p-h)!(2n_p-\lambda-g-h-1)!2^{2(n_p-g-h)}}{(n_p-\lambda-2g)!(n_p-\lambda-2h)!g!h!(2n_p-g-h+1)!} \tag{A9}$$

and $g,h$ are such that $0 \leq g,h \leq (n_p-\lambda)/2$. Adding Eqs. (A7) and (A8) we get, finally, the value for the average speed for orbital $\lambda$ given in Eq. (21).

---

*On sabbatical leave at the Department of Electrical Engineering, University of Salford, Salford M5 4WT United Kingdom.

†Centro Atómico Bariloche and Instituto Balseiro, 8400 San Carlos de Bariloche, Argentina.

[1]O. B. Firsov, Zh. Eksp. Teor. Fiz. 36, 1517 (1959) [Sov. Phys.—JETP 9, 1076 (1959)].

[2](a) J. Lindhard, K. Dan. Vidensk. Selsk. Mat.—Fys. Medd. 28, No. 8 (1954); (b) J. Lindhard and M. Scharff, Phys. Rev. 124, 128 (1961).

[3]D. J. Land, J. G. Brennan, D. G. Simons, and M. D. Brown, Phys. Rev. A 16, 492 (1977).

[4](a) I. M. Cheshire, G. Dearnaley, and J. M. Poate, Phys. Lett. A 27, 304 (1968); (b) Proc. R. Soc. London Ser. A 311, 47 (1969); (c) I. M. Cheshire and J. M. Poate, in *Atomic Collision Phenomena in Solids,* edited by D. W. Palmer, M. W. Thompson, and P. D. Townsend (North-Holland, Amsterdam, 1970), p. 351.

[5](a) J. Lindhard and A. Winther, K. Dan. Vidensk. Selsk. Mat.—Fys. Medd. 34, No. 4, (1964); (b) E. Bonderup, *ibid.* 35, No. 17 (1967); (c) W. Pietsch, U. Hauser, and W. Neuwirth, Nucl. Instrum. Methods 132, 79 (1976).

[6]S. A. Cruz, C. Vargas, and D. K. Brice, Radiat. Eff. Lett. 43, 79 (1979).

[7]S. A. Cruz, C. Vargas, and D. K. Brice, Nucl. Instrum. Methods 170, 205 (1980).

[8](a) D. K. Brice, Phys. Rev. A 6, 1791 (1972); (b) A 19, 1367 (1979).

[9]P. Gombás, *Die Statistische Theorie des Atoms und ihre Anwendungen* (Springer, London and New York, 1952).

[10]For a review, see, for example, I. A. Akhiezer and L. N. Davydov, Sov. Phys.—Usp. 22, 804 (1979) [Usp. Fiz. Nauk 129, 239 (1979)].

[11](a) C. P. Bhalla and J. N. Bradford, Phys. Lett. A 27, 318 (1968); (b) C. P. Bhalla, J. N. Bradford, and G. Reese, in Ref. 4(c), p. 361.

[12]K. B. Winterbon, Can. J. Phys. 46, 2429 (1968).

[13]A. H. El-Hoshy and J. F. Gibbons, Phys. Rev. 173, 454 (1968).

[14]S. A. Cruz, C. Cisneros, and I. Alvarez, Phys. Rev. A 17, 132 (1978); A 18, 2369 (1978); A 20, 628 (1979).

[15]U. Fano and W. Lichten, Phys. Rev. Lett. 16, 625 (1965).

[16]E. Clementi and C. Roetti, At. Data Nucl. Data Tables 14, 177 (1974).

[17]E. U. Condon and G. H. Shortley, *The Theory of Atomic Spectra* (Cambridge University, London, 1953).

[18](a) F. F. Komarov and M. A. Kumakhov, Phys. Status Solidi B 58, 380 (1973); (b) F. F. Komarov, Radiat. Eff. Lett. 43, 139 (1979).

[19]B. J. McClelland, *Statistical Thermodynamics* (Benjamin, New York, 1973), p. 297.

[20]H. Goldstein, *Classical Mechanics* (Addison-Wesley, Reading, Mass., 1950), Chap. 3.

[21]B. M. Latta and P. J. Scanlon, Phys. Status Solidi B 74, 711 (1976).
[22]N. Bohr, K. Dan. Vidensk. Selsk. Mat.—Fys. Medd. 18, No. 8 (1948).
[23]L. Brillouin, Actual. Sci. Ind. 160, (1934).
[24]See, for example, I. M. Torrens, *Interatomic Potentials* (Academic, New York, 1972).
[25]S. Kalbitzer and H. Oetzmanm, Phys. Lett. A 59, 197 (1976); Radiat. Eff. 47, 57 (1980).
[26]N. Sabelli, R. Benedek, and T. L. Gilbert, Phys. Rev. A 20, 677 (1979).
[27]S. A. Cruz, L. T. Chadderton, and J. C. Barthelat, Nucl. Instrum. Methods 191, 479 (1981).
[28]S. A. Cruz, E. V. Alonso, R. P. Walker, D. J. Martin, and D. G. Armour, Nucl. Instrum. Methods 194, 659 (1982).
[29](a) R. G. Gordon and Y. S. Kim, J. Chem. Phys. 56, 3122 (1972); (b) Y. S. Kim and R. G. Gordon, *ibid.* 60, 1842 (1974); (c) R. G. Gordon and Y. S. Kim, *ibid.* 60, 4323 (1974).
[30]W. D. Wilson, C. L. Bisson, Phys. Rev. B 3, 3984 (1971).
[31]J. P. Biersack and J. F. Ziegler, Nucl. Instrum. Methods 194, 93 (1982).
[32]W. Lenz, Z. Phys. 77, 713 (1932).
[33]H. Jensen, Z. Phys. 77, 722 (1932).
[34]W. D. Wilson, L. G. Haggmark, and J. P. Biersack, Phys. Rev. B 15, 2458 (1977).
[35]A. E. S. Green, D. Sellin, and A. S. Zachor, Phys. Rev. 184, 1 (1969).
[36]Algorithm E02ACF, Numerical Algorithm Group (NAG) computer package, University of Salford, United Kingdom.
[37]L. M. Kishenevsky, Izv. Acad. Nauk. SSR, Ser. Fiz. 26, 1410 (1962) [Bull. Acad. Sci. USSR, Phys. Ser. 26, 1433 (1962)].
[38]O. S. Oen and M. T. Robinson, Nucl. Instrum. Methods 132, 647 (1976).
[39]J. P. Poate, in *Channeling,* edited by D. V. Morgan (Wiley, New York, 1973).
[40]The derivation of Eqs. (40)—(44) stems on the assumption that the series of collision events suffered by the projectile are statistically independent, i.e., follow a Poisson distribution. A formal analysis of the role of the correlation between collisions along the projectile trajectory is out of the scope of the present paper, the interested reader is addressed to a more detailed study on this topic given by P. Sigmund, K. Dan. Vidensk. Selsk. Mat.—Fys. Medd. 40, No. 5 (1978) and E. Bonderup, *Penetration of Charged Particles Through Matter, Lecture Notes* (Institute of Physics, University of Aarhus, Denmark, 1978) (unpublished).
[41](a) E. Everhart, G. Stone, and R. J. Carbone, Phys. Rev. 99, 1287 (1955); (b) F. P. Ziemba, G. J. Lockwood, G. H. Morgan, and E. Everhart, *ibid.* 118, 1552 (1960).
[42]L. Meyer, Phys. Status Solidi B 44, 253 (1971).
[43]M. Abramowitz and I. Stegun, *Handbook of Mathematical Functions* (Dover, New York, 1970).
[44]P. Hvelplund, K. Dan. Vidensk. Selsk. Mat.—Fys. Medd. 38, No. 4 (1971).
[45]W. K. Chu, P. D. Bourland, K. H. Wang, and D. Powers, Phys. Rev. 175, 343 (1968).
[46]J. R. MacDonald, Z. Naturforsch., Teil A 21, 130 (1966).
[47]J. H. Ormrod and H. E. Duckworth, Can. J. Phys. 41, 1424 (1963).
[48]J. H. Ormrod, J. R. MacDonald, and H. E. Duckworth, Can. J. Phys. 43, 275 (1965).
[49]J. H. Ormrod, Can. J. Phys. 46, 497 (1968).
[50]D. J. Land and J. G. Brennan, Nucl. Instrum. Methods 132, 98 (1976).
[51]B. Fastrup, P. Hvelplund, and C. A. Sautter, K. Dan. Vidensk. Selsk. Mat.—Fys. Medd. 35, No. 10 (1966).
[52]P. Hvelplund and B. Fastrup, Phys. Rev. 165, 408 (1968).
[53]F. H. Eisen, Can. J. Phys. 46, 561 (1968).